ACS APPLIED ELECTRONIC MATERIALS

Letter

Cite This: ACS Appl. Electron. Mater. 2019, 1, 1367−1371

pubs.acs.org/acsaelm

Thermal Oxidation of AlInN for III-Nitride Electronic and Optoelectronic Devices

Matthew R. Peart,* Xiongliang Wei, Damir Borovac, Wei Sun, Nelson Tansu,* and Jonathan J. Wierer, Jr.*

Center for Photonics and Nanoelectronics, Department of Electrical and Computer Engineering, Lehigh University, Bethlehem, Pennsylvania 18015, United States

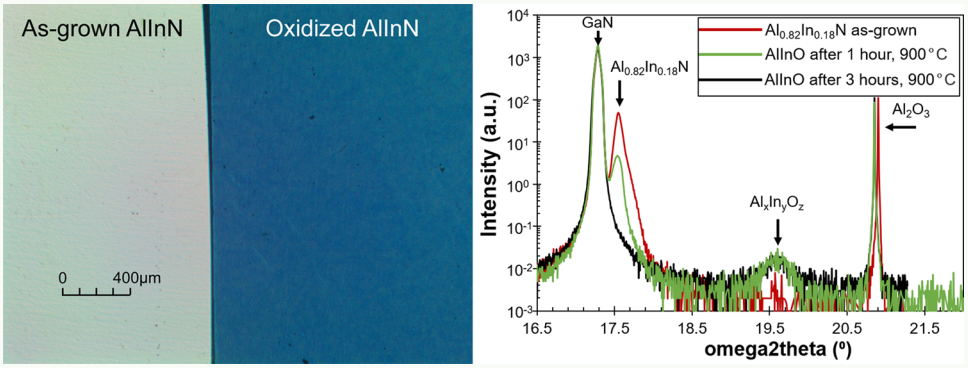

ABSTRACT: The oxidation of semiconductors is a fundamental building block of many modern electronic devices. The prime example is the oxidation of silicon into silicon dioxide, which is used as a gate dielectric, waveguides, masking layer, and a device isolation layer. The ability to form an analogous stable and insulating oxide in III-nitride semiconductors would enable a new generation of III-nitride-based electronic and optoelectronic devices. Here we present data on the conversion of thick (>100 nm) AlInN epitaxial layers into oxides with H_2O vapor in an N_2 carrier gas (wet oxidation) at elevated temperatures (900 °C). The $Al_xIn_{1-x}N$ layers are grown on and latticed-matched (x = 0.82) to GaN layers. The oxide can be formed over its entirety or selectively by patterning the surface. The conversion to an oxide is confirmed and characterized by atomic force microscopy, scanning electron microscopy, X-ray photoelectron spectroscopy, X-ray diffraction, spectroscopic ellipsometry, and electrical measurements. The oxide is smooth and crystalline, has a low index of refraction of ∼1.8 in the visible, and exhibits very high resistivity of >10^{14} Ω·cm.

KEYWORDS: *AlInN, AlInN/GaN, thermal oxidation, III-nitride oxidation, III-nitride power electronics, AlInN MOS-HEMT*

INTRODUCTION

The oxidation of semiconductors is a powerful technique that can be used to create new device architectures and processing methods. The most well-known is the oxidation of Si into SiO_2[1] that is used as an insulator, protection layer, masking layer, waveguide layer, and gate oxide. Its development into a robust oxide was key to the proliferation of Si semiconductor technology. Semiconductor oxidation is not limited to Si. The thermal oxidation of AlGaAs,[2] AlInP,[3] and AlInAs,[4] also produces successful oxides for the III-arsenide and phosphide semiconductors, and they have found uses for current confinement, photon confinement, and passivation in a wide array of optoelectronic devices.[5−7] The most successful embodiment is commercial GaAs-based vertical cavity surface emitting lasers (VCSELs) which use the oxide of AlGaAs.

A similarly successful thick oxide with high resistivity and interface morphology has yet to be demonstrated in III-nitrides although there have been some reported attempts. Thermal oxidation of GaN to form Ga_2O_3 is possible with reasonable interface state densities,[8,9] but there are significant drawbacks. Ga_2O_3 suffers from an insufficient conduction band offset and low bandgap compared to GaN, limiting its utility as an insulator or gate oxide. This oxide also has a rough interface morphology,[10,11] which also contributes to poor electrical and optical properties.[12]

Wet thermal oxidation of AlInN has yet to be reported in the literature. There have been prior demonstrations on the oxidation of AlGaN and AlInN, including the oxidation of AlGaN[13,14] and AlInN[15] in dry (O_2) atmospheres resulting in thin layers < 10 nm that are primarily for passivation and charge control in high-electron-mobility transistors (HEMTs). On the basis of these studies the prevailing notion is that Al-based III-nitride layers are limited in overall thickness. Another method of oxidation of AlInN and AlGaN is using electrochemical or anodic oxidation techniques.[16,17] This oxidation process can proceed vertically or laterally across buried AlInN

Received: April 30, 2019
Accepted: July 12, 2019
Published: July 12, 2019

DOI: 10.1021/acsaelm.9b00266
ACS Appl. Electron. Mater. 2019, 1, 1367−1371

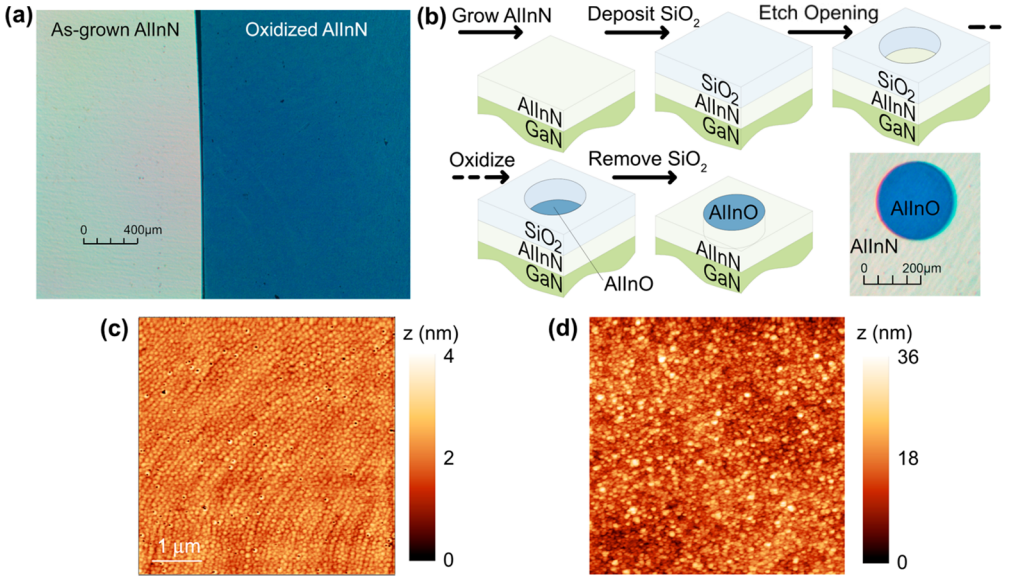

Figure 1. Top-view microscope image of (a) an as-grown, 250 nm thick $Al_xIn_{1-x}N$ layer (x = 0.82 lattice-matched to GaN) and a similar sample after wet oxidation at 900 °C for 1 h. The oxidized surface appears blue and is caused by an optical interference of the thick AlInO layer. (b) Demonstration of selective oxidation by creating circular openings in a SiO_2 mask, oxidizing the AlInN through the mask openings, and removing the SiO_2. The lower left panel shows a top-view image of the selectively oxidized circle. AFMs of the (c) as-grown AlInN layer and (d) the same layer after oxidation.

layers forming insulating layers over 10's μm. Although attractive, these electrochemical oxides are formed at low temperatures and are far different from the elevated temperature oxidation techniques successfully used in other semiconductors that result in crystalline and robust oxides.

This letter demonstrates a different approach to creating oxides in III-nitrides with promising optical and electrical characteristics. Lattice-matched $Al_xIn_{1-x}N$ (x = 0.82) layers are grown on and latticed-matched to GaN, and when exposed to conventional wet thermal oxidation (H_2O in N_2 carrier gas) at high temperatures (900 °C), they are converted to a stable and robust oxide. The oxide can be formed over the entirety of the layer or selectively by patterning the surface. The conversion to an oxide is confirmed and characterized with atomic force microscopy (AFM), scanning electron microscopy (SEM), X-ray photoelectron spectroscopy (XPS), X-ray diffraction (XRD), spectroscopic ellipsometry, and electrical measurements. The oxidation of $Al_{0.82}In_{0.18}N$ forms an oxide with high resistivity, a low refractive index, low extinction coefficients (loss), and smooth surface morphology, making it an excellent oxide to create electronic and optoelectronic devices. The resulting oxidation rates are faster and the oxide is thicker than thought possible, mainly based on previous reports that suggest only surface oxides are possible with dry O_2 oxidation.[15] The ability to form oxide layers in III-nitrides creates the possibility for new device applications such as gate oxides and optical confinement structures for waveguides.

The AlInN samples are formed by metal−organic chemical vapor deposition (MOCVD), as previously detailed,[18−20] and consist of 100 and 250 nm thick $Al_{0.82}In_{0.18}N$ layers grown on 4 μm thick unintentionally doped or n-type GaN ($n \sim 5 \times 10^{18}$ cm^{-3}) on sapphire substrates. The $Al_xIn_{1-x}N$ layers are lattice-matched to GaN (x = 0.82) as verified by X-ray diffraction (XRD) ω−2θ scans, and layer thicknesses are verified by spectroscopic ellipsometry. Hall measurement using the van der Pauw method shows the $Al_{0.82}In_{0.18}N$ layers are n-type with an electron concentration of $\sim 2 \times 10^{17}$ cm^{-3}. Oxidation consists of first cleaning with acetone and isopropyl alcohol and then placing the samples into a quartz tube furnace at a temperature of ~900 °C with N_2 flowing through an H_2O bubbler heated to 95 °C for up to 3 h. A subset of the oxidized samples with 100 nm thick $Al_{0.82}In_{0.18}N$ layers on n-type GaN layers are created to perform electrical characterization. Here the oxide is removed from a portion of the sample by a polishing process using a fine diamond grit polishing pad from opposite ends of the sample. Aluminum contacts are evaporated by electron beam evaporation both on AlInN and the oxide to compare resistivities. On the oxidized sample the resistivity between the contacts created over the polished regions was first verified to be low (<2 kΩ·cm).

Figure 1 shows images of the AlInN and oxidized AlInN layers by various microscopy techniques. Top-view microscope images are shown in Figure 1a of the as-grown and oxidized AlInN. Before oxidation, the AlInN layer is nearly transparent, typical of wide bandgap semiconductors layers of GaN and AlInN. After oxidation, AlInN is converted to an oxide that is shiny and blue in color. This deep color is due to thin film interference between the thick oxide layer and surrounding air and GaN interfaces and suggests a thick (>100 nm) oxide film forms. A simple calculation assuming a reflected peak at 470 nm confirms an oxide layer is formed with an index of ~1.8. This color change is a common observation of thin film oxide formation in other semiconductors such as Si and AlGaAs. This oxidation process is also selective as shown in the top-view microscope image in the lower left panel of Figure 1b. Here the surface is masked and patterned with SiO_2 leaving circular openings. These openings are exposed to the wet atmosphere and oxidize the surface selectively. The result is circular oxidized areas surrounded by the as-grown AlInN.

Panels c and d of Figure 2 show AFM images of the as-grown and oxidized AlInN layers, respectively. The morphology of the as-grown film is typical of lattice-matched films on GaN. It shows small circular mounds that decorate the atomic step terraces of the underlying GaN and smaller pits that are

DOI: 10.1021/acsaelm.9b00266
ACS Appl. Electron. Mater. 2019, 1, 1367−1371

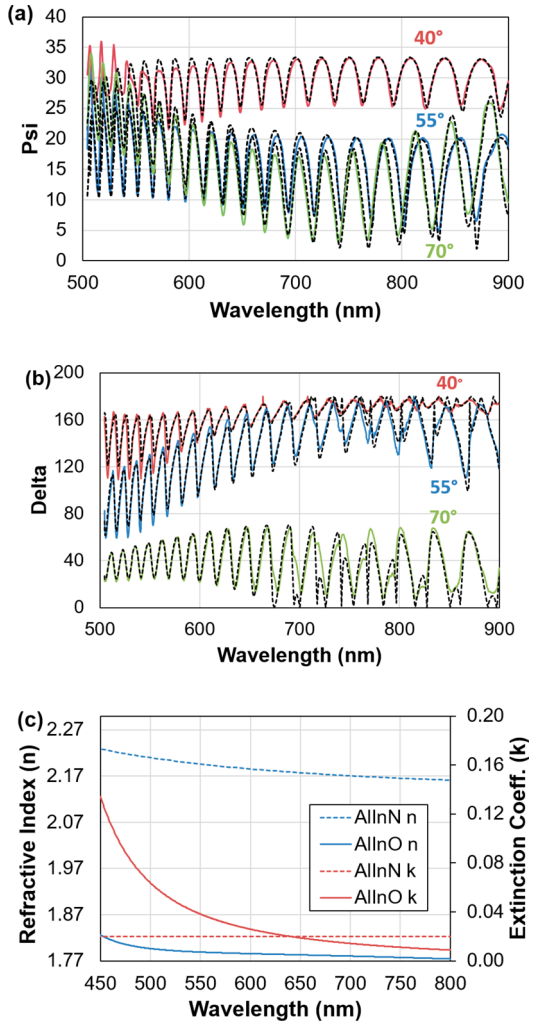

Figure 2. Ellipsometry spectra of the AlInO at three different angles (40°, 55°, and 70°) for the (a) amplitude ratio (Psi) and (b) phase difference (δ). The solid lines are the measured data, and the dotted lines are fits to the data. (c) Refractive index (n) and extinction coefficient (k) versus wavelength for the AlInO and AlInN layers determined by fitting to ellipsometry spectra. The n for the AlInO at 600 nm is ~1.79 and has low optical loss.

openings to the threading dislocations in the GaN.[21] The root mean square (RMS) roughness for these as-grown and oxidized layers are 0.5 and 4.4 nm, respectively. AFM shows that the surface of the formed oxide is relatively smooth.

Spectroscopic ellipsometry is used to estimate the thickness and optical constants of the layers before and after oxidation, and also to verify the complete conversion of the AlInN layer into an oxide. Panels a and b of Figure 2 show the amplitude ratio and phase difference of the ellipsometric spectra at three different angles. The oscillations versus wavelength are due to the thin film interferences of the oxide, AlInN, and GaN films. The thicknesses, the refractive index, n, and the extinction coefficient, k, were found by fitting the measured waveforms to the Tauc–Lorentz oscillator model. Figure 2c shows n and k for the oxide layer resulting from this fit. Across visible wavelengths, the refractive index varies from 1.77 to 1.83 and the extinction coefficient ranges from 0.01 to 0.12 for the oxide layer. Both properties increase with decreasing wavelength. The refractive index is lower than AlInN,[22] which further confirms oxidation of the layer. The low refractive index and extinction coefficient make the oxide useful for optoelectronic devices and can provide optical confinement.. The ellipsometry data also reveal the completeness of the oxidation because the sample oxidized for 1 h has an ~240 nm thick oxide layer and only an ~ 10 nm thick AlInN remaining. After 3 h of oxidation, the oxide layer has increased to the full 250 nm thickness. It is also possible to create a thinner oxide layer with shorter oxidation times.

XRD is used to verify the conversion of AlInN to an oxide. Figure 3 shows the (0002) reflections of the 250 nm thick, as-

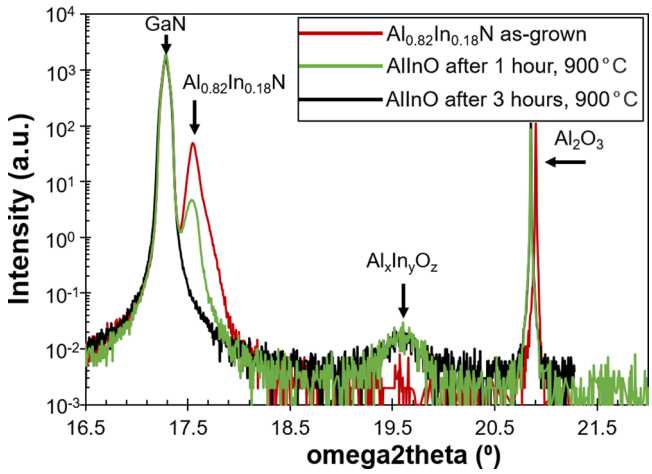

Figure 3. X-ray diffraction ω–2θ scans taken around (0002) showing reflections from the as-grown, 250 nm thick AlInN sample and AlInN samples measured after 1 and 3 h of oxidation.

grown AlInN layers and AlInN layers oxidized for 1 and 3 h. The oxidized layers are the same samples measured by spectroscopic ellipsometry. The as-grown $Al_xIn_{x-1}N$ layer shows a peak adjacent to the GaN peak at ω–2θ = 17.6°, indicating it is lattice-matched to GaN (x = 0.82). After 1 h of oxidation, the AlInN peak is lowered significantly showing weaker reflectance of the AlInN layer because it is almost completely oxidized with only ~10 nm left, consistent with the ellipsometry data. A new peak forms at ω–2θ = 19.7°, which suggest the formation of a crystalline AlInO layer. After 3 h the sample is completely oxidized as indicated by the absence of the AlInN peak. X-ray photoelectron spectroscopy (XPS), which probes the surface only, shows that wet oxidized AlInN layers have an oxygen content of greater than 50% and the remaining nitrogen is ~1%.

Figure 4 shows current versus voltage (IV) characteristics to compare the resistivity of the as-grown AlInN and the oxide layers. Samples with ohmic contacts on the as-grown AlInN and oxidized layers (inset) are prepared for the measurement. The as-grown AlInN layer is conductive, as expected, and has a resistivity of 3.3×10^3 Ω·cm. However, the oxide layer is extremely insulating with resistivities > 8×10^{14} Ω·cm, which are similar to values reported for Al_2O_3.[23] Voltage sweeps to electrical breakdown (data not shown) revealed critical electric fields > 2 MV/cm for the oxide.

The oxidation temperatures and the XRD data suggest the oxide is crystalline. To support this hypothesis, we note the oxide is also insoluble in water and the etching of the oxide using a 1:1 HF:DI solution results in no appreciable etching after 20 min. In comparison, in our studies oxides have also been formed from AlInN by dry oxidation (O_2) and

DOI: 10.1021/acsaelm.9b00266
ACS Appl. Electron. Mater. 2019, 1, 1367–1371

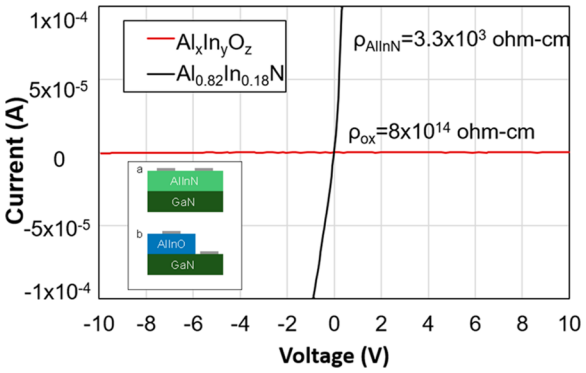

Figure 4. Plot of current versus voltage of contacted as-grown AlInN and oxidized AlInN layers on GaN. The resistivity of the oxide is extremely high compared to the AlInN layer. The inset shows the contacting scheme to the two different layers.

electrochemical methods and they both have appreciable etch rates in HF suggesting they are amorphous. Further comparing wet and dry oxidation, we observe faster oxidation rates with dry oxidation. Most likely both involve the diffusion of the oxidant through the oxide layer, and the faster dry oxidation could be due to higher diffusion of O_2 which results in a less dense oxide. The possible phases, stoichiometry, and crystallinity of Al-based oxides can be complex,[24] and the kinetics, transport, and atomic arrangement of this oxide of AlInN formed by wet oxidation require further study.

CONCLUSION

In conclusion, AlInN can be converted to an oxide when exposed to H_2O vapor in an N_2 carrier gas (wet oxidation) at elevated temperatures (900 °C). We verified this conversion with ellipsometry, XRD, XPS, and electrical testing. These promising results motivate further study of the AlInN oxide and paths toward integration in optoelectronic and electronic devices.

AUTHOR INFORMATION

Corresponding Authors

*(M.R.P.) E-mail: mrp211@lehigh.edu.
*(N.T.) E-mail: tansu@lehigh.edu.
*(J.J.W.) E-mail: jwierer@lehigh.edu.

ORCID

Matthew R. Peart: 0000-0001-9496-393X
Wei Sun: 0000-0003-2193-1456

Funding

We acknowledge funding from U.S. National Science Foundation (Award Nos. 1408051, 1505122, and 1708227), and the Daniel E. '39 and Patricia M. Smith Endowed Chair Professorship Fund (N.T.).

Notes

The authors declare no competing financial interest.

ACKNOWLEDGMENTS

We thank Dr. Henry Luftman for the XPS measurements.

REFERENCES

(1) Frosch, C. J.; Derick, L. Surface Protection and Selective Masking during Diffusion in Silicon. *J. Electrochem. Soc.* **1957**, *104* (9), 547.
(2) Dallesasse, J. M.; Holonyak, N.; Sugg, A. R.; Richard, T. A.; El-Zein, N. Hydrolyzation Oxidation of AlxGa1-XAs-AlAs-GaAs Quantum Well Heterostructures and Superlattices. *Appl. Phys. Lett.* **1990**, *57*, 2844.
(3) Cao, Y.; Zhang, J.; Li, X.; Kosel, T. H.; Fay, P.; Hall, D. C.; Zhang, X. B.; Dupuis, R. D.; Jasinski, J. B.; Liliental-Weber, Z. Electrical Properties of InAlP Native Oxides for Metal-Oxide-Semiconductor Device Applications. *Appl. Phys. Lett.* **2005**, *86*, 062105−062107.
(4) Petit, P.; Legay, P.; Le Roux, G.; Patriarche, G.; Post, G.; Quillec, M. Controlled Steam Oxidation of AlInAs for Microelectronics and Optoelectronics Applications. *J. Electron. Mater.* **1997**, *26* (12), L32−L35.
(5) Huffaker, D. L.; Deppe, D. G.; Kumar, K.; Rogers, T. J. Native-Oxide Defined Ring Contact for Low Threshold Vertical-Cavity Lasers. *Appl. Phys. Lett.* **1994**, *65* (1), 97−99.
(6) Maranowski, S. A.; Sugg, A. R.; Chen, E. I.; Holonyak, N. Native Oxide Top- and Bottom-Confined Narrow Stripe p-n Al YGa1-YAs-GaAs-InxGa1-XAs Quantum Well Heterostructure Laser. *Appl. Phys. Lett.* **1993**, *63*, 1660.
(7) Wierer, J. J.; Evans, P. W.; Holonyak, N.; Kellogg, D. A. Vertical Cavity Surface Emitting Lasers Utilizing Native Oxide Mirrors and Buried Tunnel Contact Junctions. *Appl. Phys. Lett.* **1998**, *72* (21), 2742−2744.
(8) Kim, H.; Park, S.-J.; Hwang, H. Thermally Oxidized GaN Film for Use as Gate Insulators. *J. Vac. Sci. Technol., B: Microelectron. Process. Phenom.* **2001**, *19* (2), 579.
(9) Nakano, Y.; Jimbo, T. Interface Properties of Thermally Oxidized n -GaN Metal−oxide−semiconductor Capacitors. *Appl. Phys. Lett.* **2003**, *82* (2), 218−220.
(10) Korbutowicz, R.; Prazmowsk, J. Wet Thermal Oxidation of GaAs and GaN. *Semicond. Technol.* **2010**, 257−260.
(11) Brona, J.; Grodzicki, M.; Ciszewski, A.; Zuber, S.; Mazur, P. Oxidation of GaN(0001) by Low-Energy Ion Bombardment. *Appl. Surf. Sci.* **2014**, *304*, 20−23.
(12) Yamada, T.; Ito, J.; Asahara, R.; Watanabe, K.; Nozaki, M.; Hosoi, T.; Shimura, T.; Watanabe, H. Improved Interface Properties of GaN-Based Metal-Oxide-Semiconductor Devices with Thin Ga-Oxide Interlayers. *Appl. Phys. Lett.* **2017**, *110* (26), 261603.
(13) Roccaforte, F.; Giannazzo, F.; Iucolano, F.; Bongiorno, C.; Raineri, V. Two-Dimensional Electron Gas Insulation by Local Surface Thin Thermal Oxidation in AlGaN/GaN Heterostructures. *Appl. Phys. Lett.* **2008**, *92* (25), 252101.
(14) Mistele, D.; Rotter, T.; Röver, K. S.; Paprotta, S.; Seyboth, M.; Schwegler, V.; Fedler, F.; Klausing, H.; Semchinova, O. K.; Stemmer, J.; Aderhold, J.; Graul, J. First AlGaN/GaN MOSFET with Photoanodic Gate Dielectric. *Mater. Sci. Eng., B* **2002**, *93*, 107−111.
(15) Eickelkamp, M.; Weingarten, M.; Rahimzadeh Khoshroo, L.; Ketteniss, N.; Behmenburg, H.; Heuken, M.; Kalisch, H.; Jansen, R. H.; Vescan, A. On the Thermal Oxidation of AlInN/AlN/GaN Heterostructures. *Phys. Status Solidi Curr. Top. Solid State Phys.* **2011**, *8* (7−8), 2213−2215.
(16) Harada, N.; Hori, Y.; Azumaishi, N.; Ohi, K.; Hashizume, T. Formation of Recessed-Oxide Gate for Normally-off AlGaN/GaN High Electron Mobility Transistors Using Selective Electrochemical Oxidation. *Appl. Phys. Express* **2011**, *4* (2), 021002.
(17) Dorsaz, J.; Bühlmann, H. J.; Carlin, J. F.; Grandjean, N.; Ilegems, M. Selective Oxidation of AlInN Layers for Current Confinement in III-Nitride Devices. *Appl. Phys. Lett.* **2005**, *87* (7), 072102.
(18) Zhang, J.; Tong, H.; Liu, G.; Herbsommer, J. A.; Huang, G. S.; Tansu, N. Characterizations of Seebeck Coefficients and Thermoelectric Figures of Merit for AlInN Alloys with Various In-Contents. *J. Appl. Phys.* **2011**, *109* (5), 053706.
(19) Tong, H.; Zhang, J.; Liu, G.; Herbsommer, J. A.; Huang, G. S.; Tansu, N. Thermoelectric Properties of Lattice-Matched AlInN Alloy Grown by Metal Organic Chemical Vapor Deposition. *Appl. Phys. Lett.* **2010**, *97* (11), 112105.

DOI: 10.1021/acsaelm.9b00266
ACS Appl. Electron. Mater. 2019, 1, 1367−1371

(20) Zhang, J.; Kutlu, S.; Liu, G.; Tansu, N. High-Temperature Characteristics of Seebeck Coefficients for AlInN Alloys Grown by Metalorganic Vapor Phase Epitaxy. *J. Appl. Phys.* **2011**, *110* (4), 043710.
(21) Chung, R. B.; Wu, F.; Shivaraman, R.; Keller, S.; Denbaars, S. P.; Speck, J. S.; Nakamura, S. Growth Study and Impurity Characterization of AlxIn 1-XN Grown by Metal Organic Chemical Vapor Deposition. *J. Cryst. Growth* **2011**, *324*, 163−167.
(22) Aschenbrenner, T.; Dartsch, H.; Kruse, C.; Anastasescu, M.; Stoica, M.; Gartner, M.; Pretorius, A.; Rosenauer, A.; Wagner, T.; Hommel, D. Optical and Structural Characterization of AlInN Layers for Optoelectronic Applications. *J. Appl. Phys.* **2010**, *108* (6), 063533.
(23) Shackelford, J. F.; Alexander, W. *Materials Science and Engineering Handbook*, 3rd ed.; CRC Press: Boca Raton, FL, USA, 2001.
(24) Wefers, K.; Misra, C. *Oxides and Hydroxides of Aluminum*, Alcoa Technical Paper No. 19; Aluminum Company of America (Alcoa): Pittsburgh, PA, USA, 1987

DOI: 10.1021/acsaelm.9b00266
ACS Appl. Electron. Mater. 2019, 1, 1367−1371